

# Phase and state transition effects on dielectric, mechanical, and thermal properties of polyols

Riku A. Talja<sup>a</sup>, Yrjö H. Roos<sup>b,\*</sup>

<sup>a</sup>Department of Food Technology, University of Helsinki, P.O. Box 27, Latokartanonkaari 7, 00014 Helsinki, Finland

<sup>b</sup>Department of Food Science, Food Technology and Nutrition, University College Cork, Cork, Ireland

## Abstract

The present study investigated the glass transition, crystallisation and melting behaviour of erythritol, xylitol, and glucitol (sorbitol) using dielectric analysis (DEA), differential scanning calorimetry (DSC), and dynamic mechanical analysis (DMA). Sorbitol and xylitol were plasticised by water and their glass transition temperatures decreased when water content was increased. Erythritol crystallised rapidly, and its water plasticisation behaviour could not be determined. Melting of the crystalline polyols occurred at their specific melting temperatures. Melts of erythritol and xylitol crystallised on recooling and no glass transition was apparent on reheating. Quench cooled sorbitol melt remained amorphous and showed a glass transition on reheating. Glass transition and crystallisation were apparent in the DSC thermogram and the dielectric and the dynamic mechanical spectra of mixtures of amorphous and crystalline xylitol. © 2001 Elsevier Science B.V. All rights reserved.

**Keywords:** Crystallisation; Dielectric analysis; Differential scanning calorimetry; Dynamic mechanical analysis; Glass transition; Melting; Polyols; Relaxations; Water

## 1. Introduction

Polyols, such as erythritol, xylitol and glucitol (sorbitol), have become important in food and pharmaceutical applications, as they are increasingly used to provide sweetness to various products or replace sugar in confectionery. These polyols have the characteristic sweet taste of sugars but the amount of energy (calories) in the products is reduced as compared with the use of sucrose [1–3]. Another important advantage is that they do not contribute to the development of dental caries [1,2,4]. Moreover, these polyols are suitable for diabetics, because they do not require insulin or glucose in their metabolism [1,4].

In industrial applications, the state and phase transitions [5] of the polyols affect their molecular mobility and physicochemical properties, for example, formation of structure, structural changes, time-dependent crystallisation and product shelf life [6]. The most important state transition of polyols and other low molecular weight carbohydrates is the glass transition. The glass transition refers to the change in state of an amorphous material in a supercooled or supersaturated state. Such materials may exhibit solid and brittle, glass-like properties or they may behave like highly viscous liquids with rubbery, leathery, or syrup-like properties. The transition between these states occurs over a temperature range that is referred to as the glass transition. The glass transition of glucose was studied in detail in one of the first series of studies of glass transitions of sugars [7]. The glass transition of the corresponding polyol, sorbitol, was

\* Corresponding author. Tel.: +353-21-4902386;

fax: +353-21-4270213.

E-mail address: yrjo.roos@ucc.ie (Y.H. Roos).

paid attention to because of its convenient glass transition of  $-9^{\circ}\text{C}$  that allowed detection of relaxations in the vicinity of the transition [8]. As the industrial uses of polyols have increased, there is also a need for detailed knowledge of their behaviour in the amorphous state. The amorphous state is a non-equilibrium state and the time-dependent changes, including crystallisation, may contribute to processing requirements and shelf life of products containing amorphous carbohydrates as components [9]. For example, the glass transition of freeze-concentrated solutions affects material behaviour, collapse properties, and processing requirements in freeze-drying [10,11]. Lactose is another example of a material exhibiting time-dependent crystallisation during storage of lactose-containing products [12–14].

Sucrose is probably the most studied low molecular weight carbohydrate and several state diagrams with detailed information of the water plasticisation behaviour as well as the transitions in the freeze-concentrated state of sucrose have been published [15–17]. Roos [18] studied the glass transitions of monosaccharides and disaccharides, including polyols. It was found that all materials were significantly plasticised by water. Furthermore, the glass transitions of the materials increased with increasing molecular weight, but there were significant differences in the transition temperatures between individual monosaccharides and disaccharides. In the present study, we used various thermal analytical techniques to analyse the glass transition, water plasticisation, and crystallisation behaviour of common polyols as well as dielectric and mechanical relaxations in the vicinity of the glass transition.

## 2. Experimental

### 2.1. Sample preparation

Erythritol (>99.5% purity) (149-32-6), from Cere-star International (Neuilly-sur-Seine, France) and xylitol (>99% purity) (87-99-0), and sorbitol (>97% purity) (50-70-4) from Roquette Frères (Lestrem, France) were prepared to an amorphous, anhydrous state by heating of the crystalline polyols above their respective melting temperatures followed by quench cooling. Amorphous, anhydrous polyols used in the differential scanning calorimetry (DSC) measurements

were prepared by melting and subsequent cooling in the DSC measuring cell. In DSC, the crystalline polyol samples (8–14 mg) were equilibrated first at the starting temperature. The samples were subsequently heated to above their respective melting temperature to produce a liquid melt. Amorphous, anhydrous samples for dielectric analysis (DEA) and dynamic mechanical analysis (DMA) were prepared by heating the crystalline polyol ( $\sim 10$  g) in a beaker to above the melting temperature until a clear melt was obtained. The polyol melt was quench cooled to room temperature and a sample was prepared and placed gently with a glassrod on to the DEA plate ( $\sim 0.5$  ml) or poured in to the DMA sample holder ( $\sim 4$  ml). The chemical structures of the polyols are presented in Fig. 1 [4,19]. Polyols with different water contents (10, 20, 30 and 40%) were produced by adding the corresponding amount of water (1–2.5 g) to the crystalline polyol (3–4.5 g) and a gentle heating was applied to melt the polyol crystals in a beaker under manual stirring. Heating was applied until a clear melt was obtained and the sample was cooled to room temperature. The exact water contents of the polyol samples were determined gravimetrically on an analytical balance. Polyol tablets, diameter 24 mm and thickness 1 mm, were used in the DEA measurements. These were prepared by compressing 0.6 g of the crystalline materials under 20 tonnes pressure for 5 min using a pressing cylinder and a piston. Compression process did not change relaxation and melting temperatures of

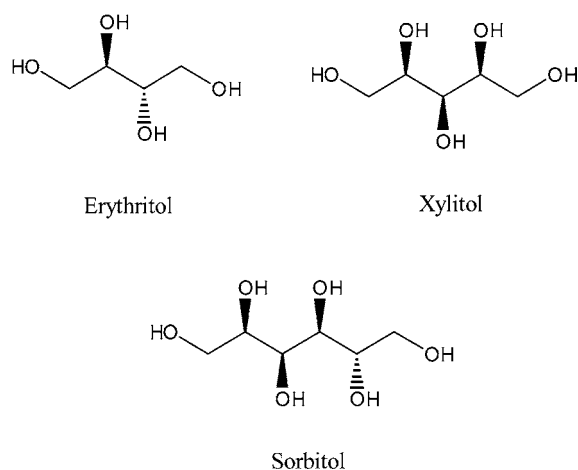


Fig. 1. Chemical structure of erythritol, glucitol (sorbitol), and xylitol.

samples. Mixtures of amorphous and crystalline xylitol were prepared by adding 1% (w/w) of crystalline xylitol (0.1 g) at room temperature into the amorphous anhydrous xylitol (9.9 g), prepared as the amorphous anhydrous samples for DEA and DMA. The crystalline xylitol was mixed gently using a glass rod with the amorphous anhydrous xylitol.

## 2.2. Differential scanning calorimetry

A differential scanning calorimeter (TA4000 DSC30, Mettler-Toledo AG) was used to determine the glass transition temperature,  $T_g$ , and the crystallisation and melting behaviour of the polyols with different water contents. DSC was calibrated using melting temperatures and enthalpies of *n*-pentane ( $-129.7^\circ\text{C}$ ;  $116.7 \text{ J g}^{-1}$ ), *n*-hexane ( $-95^\circ\text{C}$ ;  $151.8 \text{ J g}^{-1}$ ), mercury ( $-38.8^\circ\text{C}$ ;  $11.4 \text{ J g}^{-1}$ ), distilled water ( $0^\circ\text{C}$ ;  $334.5 \text{ J g}^{-1}$ ), gallium ( $29.8^\circ\text{C}$ ;  $80 \text{ J g}^{-1}$ ), and indium ( $156.6^\circ\text{C}$ ;  $28.5 \text{ J g}^{-1}$ ). Distilled water was included in calibration, because it has a well defined melting point and enthalpy. This with the other substances confirmed the validity of calibration over a wide temperature and heat flow range. DSC was used at a heating rate of  $5^\circ\text{C min}^{-1}$  and the dynamic temperature range varied from  $-140$  to  $140^\circ\text{C}$ , depending on the sample. Temperature ranges for individual samples are listed in Table 1. Crystalline polyol samples were hermetically sealed in  $40 \mu\text{l}$  aluminium pans (Mettler-27331). The sample weights were 8–14 mg and 2–4 mg for glass transition and melting temperature determinations, respectively. A flow of dry  $\text{N}_2$  ( $50 \text{ ml min}^{-1}$ ) was used to purge the measuring cell and prevent water condensation. Three replicate samples were analysed. The glass transition

and melting temperatures were taken from the onset temperatures of the endothermic transitions [6].

## 2.3. Dielectric analysis

A dielectric analyser (DEA 2970, TA Instruments) was used to study changes in the physical state by observing the permittivity  $\epsilon'$ , loss factor  $\epsilon''$ , and ratio of loss factor to permittivity  $\epsilon''/\epsilon'$  (dissipation factor,  $\tan \delta$ ), as a function of temperature. The  $\epsilon'$  describes an alignment of dipoles and the  $\epsilon''$  describes an energy that is required to align dipoles. A maximum of the  $\epsilon''/\epsilon'$  peak at 0.1 Hz was taken as the glass transition temperature,  $T_g$ , to compare with results from other techniques. Dielectric data were collected during dynamic heating at a heating rate of  $2^\circ\text{C min}^{-1}$  from  $-150$  to  $140^\circ\text{C}$ . The frequencies used were 0.1, 0.5, 1, 5, 10, 20, 50, 100 and 1000 Hz. A parallel plate mode was used with parallel plate sensors to evaluate dielectric properties of amorphous and crystalline polyol samples and the mixture of the amorphous and crystalline xylitol. A flow of  $\text{N}_2$  ( $50 \text{ ml min}^{-1}$ ) was used to purge the measuring cell and prevent water condensation on the measuring head and sample. Three replicate samples were analysed.

## 2.4. Dynamic mechanical analysis

A dynamic mechanical analyser (DMA 242, Netzsch-Gerätenbau GmbH) was used to study the  $\alpha$ -relaxation (glass transition) by observing the storage modulus  $E'$ , loss modulus  $E''$ , and  $\tan \delta$ , as a function of temperature. A maximum in the  $E''$  peak at 1 Hz was taken as the glass transition temperature,  $T_g$ , to compare with results from other techniques. The DMA data were collected at a heating rate of  $2^\circ\text{C min}^{-1}$  from  $-120$  to  $50^\circ\text{C}$ . Frequencies used were 1, 2.5, 5, 10 and 20 Hz, and the amplitude was  $15 \mu\text{m}$ . For amorphous polyols, a disk-bending sample holder adapted from MacInnes [20], as described by Laaksonen and Roos [21], was used. The disk-bending sample holder consist of a set of three stainless steel sheets with circular holes with 30 and 26 mm diameters. The three sheets were in layers where the sheet with 30 mm hole was placed in the middle and covered with plastic film on both sides. Samples of amorphous and the mixture of amorphous and crystalline xylitol were placed in the disk-bending sample holder

Table 1  
Temperature ranges of DSC measurements

Material	Temperature ( $^\circ\text{C}$ )	
	Start	End
Erythritol	-75	140
Sorbitol	-50	120
Sorbitol with water 10–40%	-140	120
Xylitol	-50	120
Xylitol with water 10–40%	-140	120
Amorphous xylitol with 1% (w/w) crystalline xylitol	-100	120

between the two plastic films. Three replicate samples were analysed.

### 3. Results and discussion

#### 3.1. Glass transition

Polyols tend to crystallise fairly rapidly from the amorphous state at temperatures higher than the glass transition temperature [18]. In the present study, erythritol was found to crystallise rapidly from an erythritol melt. A DSC cooling rate of  $5^{\circ}\text{C min}^{-1}$  was found to allow complete crystallisation and no glass transition was apparent in a subsequent reheating scan. However, samples quench cooled using the highest applicable cooling rate (approximately  $50^{\circ}\text{C min}^{-1}$ ) gave a glass transition of  $-45^{\circ}\text{C}$  in an immediate rescan. The glass transition was followed by a crystallisation exotherm occurring over a temperature range from  $-10$  to  $5^{\circ}\text{C}$ . The onset of the endothermic melting of the crystals formed was at  $118^{\circ}\text{C}$  (Table 2). This was the same temperature as was found for initial melting of crystals and agreed with that ( $117.8^{\circ}\text{C}$ ) reported by Barone et al. [22].

Amorphous xylitol and sorbitol were found to have a glass transition with onset at  $-24$  and  $-6^{\circ}\text{C}$ , respectively. These temperatures differed to some extent from those reported for xylitol ( $-19^{\circ}\text{C}$ ) by Orford et al. [23] and for sorbitol ( $-5^{\circ}\text{C}$ ) by Murthy [24]. The melting temperatures for anhydrous, crystalline xylitol and sorbitol were at  $93$  and  $95^{\circ}\text{C}$ , respectively (Table 2). Barone et al. [22] reported melting temperatures of  $92.6$  and  $93.4^{\circ}\text{C}$  for xylitol and sorbitol, respectively. The temperature difference between the glass transition temperature and the melting temperature or, preferably, the temperature ratio of  $T_m/T_g$  can

be used as a measure of the tendency for crystallisation from the amorphous state. Generally, carbohydrates with high  $T_m/T_g$  ratios are readily crystallisable [9] and have a high heat of fusion [25].  $T_m/T_g$  ratios for polyols were calculated and are given in Table 2. The  $T_m/T_g$  ratio for erythritol was clearly higher than those of xylitol and sorbitol. The data showed that the temperature difference between the  $T_g$  and  $T_m$  was large being  $163^{\circ}\text{C}$  and giving a  $T_m/T_g$  ratio of 1.71. This ratio is extremely high and agrees with the observed high tendency of erythritol to crystallise from the amorphous state. In an earlier study, Roos [18] found that the  $T_m/T_g$  ratios were 1.48 for xylitol, 1.36 for sorbitol, but within the range 1.33–1.37 for most sugars. Moreover, the latent heat of melting of erythritol was substantially higher than that of the other polyols and those reported for sugars [18].

The glass transitions of sorbitol and xylitol decreased with increasing water content. Typical DSC heating thermograms for rapidly cooled sorbitol and xylitol with different water contents (0, 10, 20, 30 and 40%) are shown in Fig. 2. The observed water plasticisation resulted from an increase in the free volume of the material allowing a higher molecular mobility for the polyol molecules. As a consequence, the  $T_g$  was decreased to a lower temperature [6]. The 40% solutions showed a typical devitrification (ice formation) exotherm followed by an ice melting endotherm of rapidly cooled sugar solutions. In general, ice formation in amorphous carbohydrates requires more than 20% (w/w) of water. However, ice formation is delayed in highly concentrated solutions and rigorous annealing treatments are required for ice formation. In the present study, the ice formation most likely resulted from ice nucleation at low temperatures and as the rapidly cooled solutions were heated to above the glass transition ice crystallisation

Table 2

Glass transition temperature ( $T_g$ ) (onset), change in heat capacity ( $\Delta C_p$ ) over the glass transition temperature range, melting temperature ( $T_m$ ) (onset), latent heat of melting ( $\Delta H_m$ ), and the  $T_m/T_g$  ratio for the polyols (mean value  $\pm$  S.D. from three measurements)

	$T_g$ ( $^{\circ}\text{C}$ )	$\Delta C_p$ ( $\text{J g}^{-1} \text{K}^{-1}$ )	$T_m$ ( $^{\circ}\text{C}$ )	$\Delta H_m$		$T_m/T_g$
				In $\text{J g}^{-1}$	In $\text{kJ mol}^{-1}$	
Erythritol	$-44.9 \pm 0.5$	$1.02 \pm 0.03$	$118 \pm 0.3$	$315 \pm 1$	38	1.71
Sorbitol	$-6 \pm 0.6$	$0.94 \pm 0.02$	$95 \pm 1.2$	$165 \pm 1$	30	1.38
Xylitol	$-24.1 \pm 0.1$	$0.97 \pm 0.02$	$92.7 \pm 0.1$	$232 \pm 1$	35	1.48

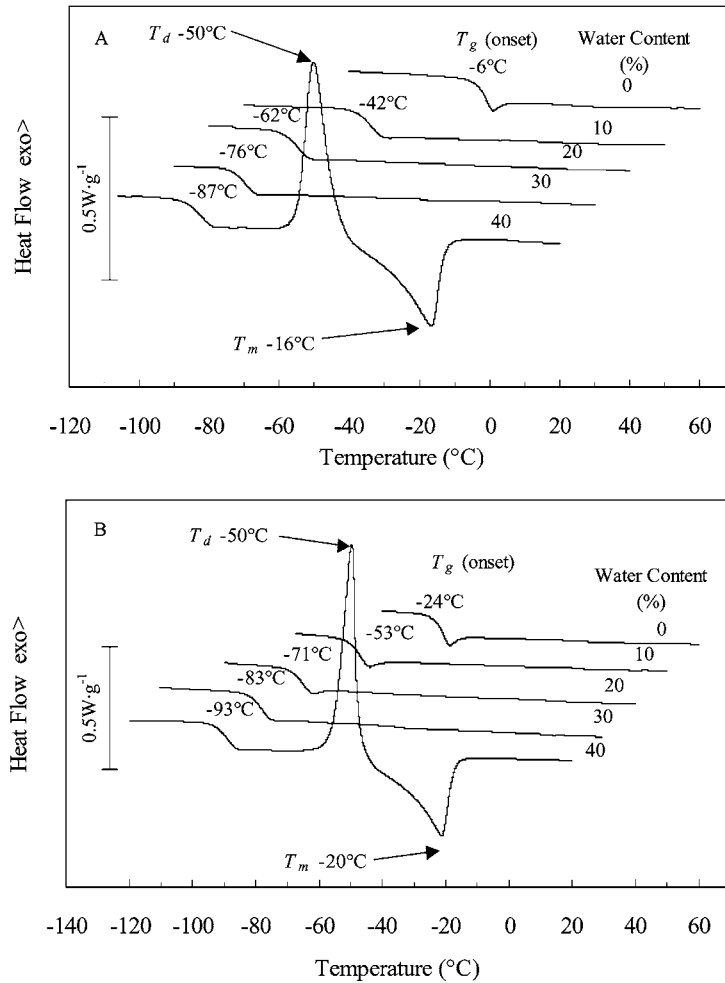


Fig. 2. Typical DSC thermograms for amorphous (A) sorbitol and (B) xylitol at different water contents showing glass transition ( $T_g$ ) and at high water contents ice formation during rewarming (devitrification,  $T_d$ ) and ice melting endotherm ( $T_m$ ). The scanning rate was  $5^\circ\text{C} \text{ min}^{-1}$ .

occurred and the devitrification endotherm was apparent in the DSC thermograms.

### 3.2. Dielectric relaxations

Detection of  $\alpha$ -relaxation temperature from DEA spectra used locating a maximum in a  $\epsilon''/\epsilon'$  ( $\tan \delta$ ) peak, as shown in Fig. 3. The  $\alpha$ -relaxation peak appears when molecules are rotating in phase with the applied frequency [26]. At a low frequency, molecules are able to follow an oscillating electric field more easily than at higher frequency and the maximum indicating  $\alpha$ -relaxation is shifted to higher

temperatures with increasing frequency. The  $\alpha$ -relaxation with different frequencies were modelled for sorbitol and xylitol using the Arrhenius relationship of Eq. (1) where  $f$  is the frequency,  $A$  is a constant,  $R$  the gas constant, and  $T$  is the absolute temperature of the  $\alpha$ -relaxation peak.

$$\ln f = \ln A - \frac{E_a}{RT} \quad (1)$$

The activation energy  $E_a$ , was obtained from the slope of the linear regression line and values of 312 and  $402 \text{ kJ mol}^{-1}$  and  $r^2$  values of regression lines of 0.984 and 0.993 for xylitol and sorbitol, respectively,

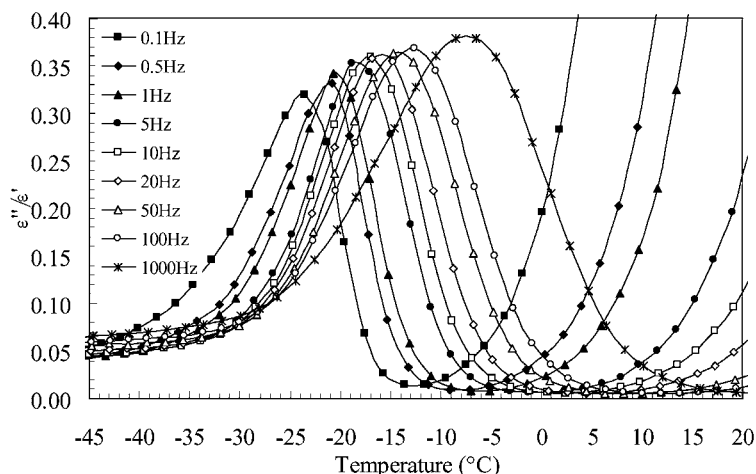


Fig. 3. Typical dielectric spectra ( $\tan \delta = \epsilon''/\epsilon'$ ) of amorphous xylitol over the glass transition temperature range at various frequencies. The data were obtained using dynamic heating at  $2^\circ\text{C min}^{-1}$ .

were obtained. The Arrhenius plots of  $\ln f$  as a function of the reciprocal absolute temperature are shown in Fig. 4. It appeared that frequencies of 0.05 and 0.12 Hz for sorbitol and xylitol, respectively, agreed with the glass transition temperature measured using DSC. In the present study, the  $\alpha$ -relaxation of  $-24^\circ\text{C}$  for xylitol and  $-5^\circ\text{C}$  for sorbitol was detected at 0.1 Hz frequency. Noel et al. [27] reported  $\alpha$ -relaxation values of  $-14^\circ\text{C}$  for xylitol and  $10.5^\circ\text{C}$  for sorbitol as measured by DEA using a 1 kHz frequency and a heating rate of  $1^\circ\text{C min}^{-1}$ . Our results gave the  $\alpha$ -relaxation values of  $-6^\circ\text{C}$  for xylitol and  $13^\circ\text{C}$  for sorbitol at 1 kHz frequency and a heating rate of  $2^\circ\text{C min}^{-1}$ . The difference in the  $\alpha$ -relaxation values of Noel et al. [27] and the present study may reflect the difference in the dynamic heating rates, as the slower heating rate may be expected to be more sensitive for detecting changes in the  $\alpha$ -relaxation and shift the observed relaxation peak to a lower temperature. However, it may be assumed that the most appropriate measurements should be carried out isothermally using several frequencies. The  $\alpha$ -relaxation of erythritol melt could not be determined in the present study due to the rapid crystallisation behaviour of erythritol.

### 3.3. Dynamic mechanical behaviour

Fig. 5 shows plots of  $E'$  and  $E''$  as a function of temperature at frequencies of 1–20 Hz for amorphous,

anhydrous sorbitol. In the DMA, the energy is imparted by applying oscillating forces. The material becomes less rigid at the  $\alpha$ -relaxation temperature and  $E'$  decreases, and  $E''$  increases as a result of absorption of applied energy [5]. Detection of the  $\alpha$ -relaxation temperature from DMA spectra used a maximum in the  $E''$  peak. In DMA measurements, we observed a corresponding frequency dependence of the  $\alpha$ -relaxation as in the DEA study. The Arrhenius plots for sorbitol and xylitol are shown in Fig. 4. The  $E_a$  values of 258 and  $396\text{ kJ mol}^{-1}$  and  $r^2$  values of 0.981 and 0.991 for xylitol and sorbitol, respectively, were obtained. The frequencies corresponding to the calorimetric glass transition onset temperature measured by DSC, were 0.08 and 0.34 Hz for sorbitol and xylitol, respectively.

### 3.4. Water plasticisation

The  $T_g$  decrease with water plasticisation was modelled for sorbitol and xylitol using the Gordon–Taylor Eq. (2) [28] with  $T_{g1}$ -values given in Table 3 for anhydrous sorbitol and xylitol, measured by various techniques, and  $T_{g2}$  of  $-135^\circ\text{C}$  for water [29].

$$T_g = \frac{w_1 T_{g1} + k w_2 T_{g2}}{w_1 + k w_2} \quad (2)$$

The  $k$ -values obtained are summarised in Table 4. Roos reported [18] slightly different  $k$  values of 2.76 for xylitol and 3.35 for sorbitol derived from DSC

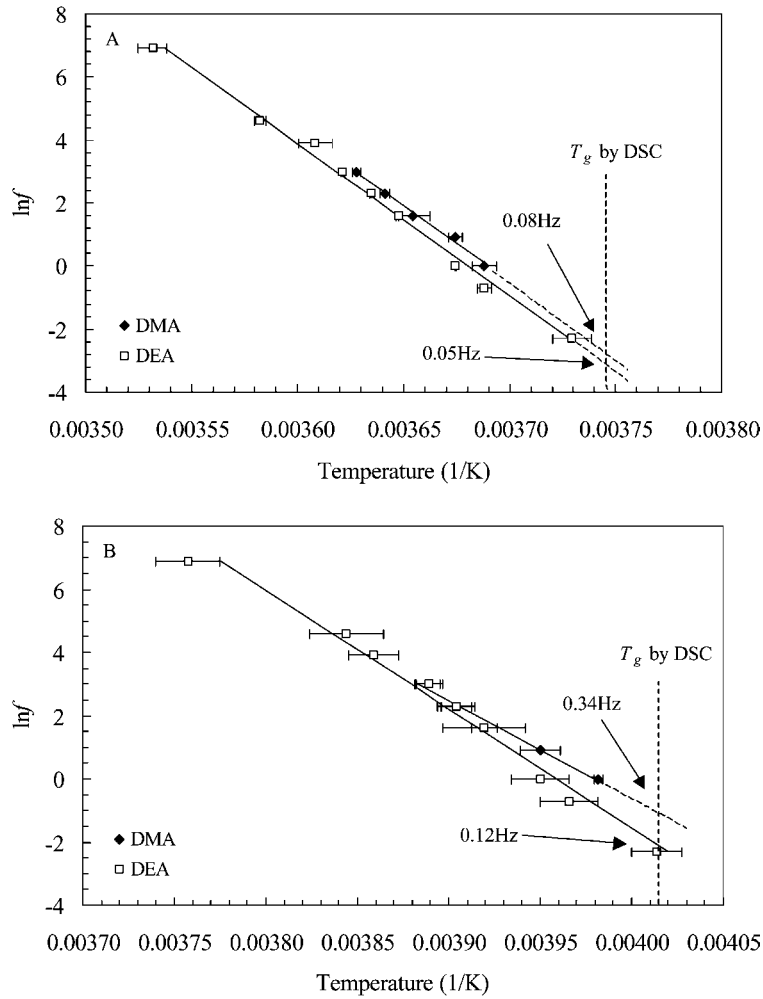


Fig. 4. Arrhenius plots of the  $\tan \delta$  peak of the dielectric and the  $E''$  peak of the mechanical spectra for (A) sorbitol and (B) xylitol obtained using dynamic heating at  $2^\circ\text{C min}^{-1}$ . The solid lines follow the Arrhenius Eq. (1) fitted to the experimental values shown. Vertical dotted line describes  $T_g$  as measured by DSC. Intersection points of vertical line and Arrhenius plots of DEA and DMA give a frequency which is correlating with  $T_g$  measured by DSC.

Table 3

Glass transition temperatures ( $T_g$ ) for sorbitol and xylitol at various water contents, as measured by DEA (temperature at  $\epsilon''/\epsilon'$  peak at 0.1 Hz), DMA (temperature at  $E''$  peak at 1 Hz), and DSC (onset temperature) (mean value  $\pm$  S.D. from three measurements)

	Sorbitol (%)					Xylitol (%)				
	100	90	80	70	60	100	90	80	70	60
DEA	$-4.8 \pm 0.7$	$-39.8 \pm 0.7$	$-61.2 \pm 0.2$	$-75.3 \pm 0.3$	$-82 \pm 0.7$	$-24.4 \pm 0.8$	$-52.2 \pm 0.7$	$-70.1 \pm 0.8$	$-84.8 \pm 0.4$	$-94.8 \pm 0.9$
DMA	$-1.9 \pm 0.4$	$-31.8 \pm 0.8$	$-54.4 \pm 0.8$	$-67.7 \pm 0.7$	$-86 \pm 0.6$	$-22.1 \pm 0.2$	$-45.6 \pm 0.8$	$-71.9 \pm 0.4$	$-78.3 \pm 0.3$	$-92.4 \pm 1.2$
DSC	$-6 \pm 0.6$	$-42.1 \pm 0.7$	$-61.7 \pm 0.8$	$-76 \pm 0.7$	$-86.9 \pm 0.3$	$-24.1 \pm 0.1$	$-53.1 \pm 0.3$	$-70.5 \pm 1.5$	$-83.3 \pm 0.6$	$-93 \pm 0.2$

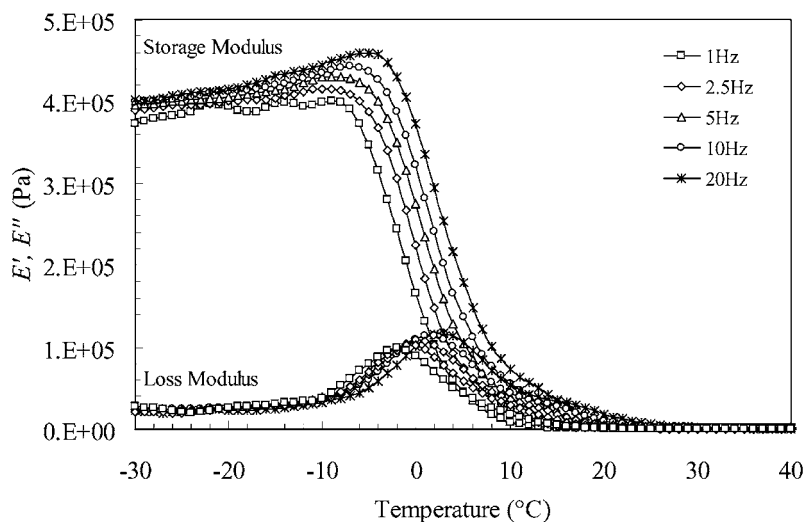


Fig. 5. Typical storage modulus ( $E'$ ) and loss modulus ( $E''$ ) spectra for amorphous sorbitol at various frequencies. The data were obtained using dynamic heating at  $2^\circ\text{C min}^{-1}$ .

data. Fig. 6 shows the Gordon–Taylor plots with experimental values for sorbitol and xylitol. The Gordon–Taylor plots showing predicted transition temperatures for various techniques were slightly different. However, the correlation was fairly high between DSC and DEA results at selected frequencies, but the DMA-value showed the largest deviation. The  $\alpha$ -relaxation temperature in the DMA results at 1 Hz frequency was taken as the  $T_g$ . However, the estimates of the frequencies correlating with the  $T_g$  measured by DSC were 0.08 and 0.34 Hz for sorbitol and xylitol, respectively, as shown in Fig. 4. The  $\alpha$ -relaxation temperature is frequency-dependent and, therefore, the selected frequency affects the observed temperature of the  $\alpha$ -relaxation.

The glass transition temperatures, as derived from DEA, DMA and DSC data, for sorbitol and xylitol, are

Table 4

The Gordon–Taylor  $k$ -value (Eq. (2)) for sorbitol and xylitol derived from experimental data obtained using various techniques (mean value  $\pm$  S.D. from three measurements)

	$k$ -value	
	Sorbitol	Xylitol
DEA	$2.81 \pm 0.48$	$2.84 \pm 0.18$
DMA	$2.51 \pm 0.16$	$2.58 \pm 0.39$
DSC	$2.96 \pm 0.42$	$2.81 \pm 0.32$

given in Table 3. These transition temperatures were slightly different between the different techniques. In an earlier study, Williams [26] concluded that the results of DEA, DMA, and DSC glass transition measurements for seeds agreed in general, but differed in detail. It should also be remembered that the glass transition is a relaxation process and the DMA and DEA results are highly dependent on the measurement frequencies. Therefore, various methods of measurement do not represent similar observation times and the results may not be comparable. In addition, the results obtained are dependent on the heating rates used and they may also depend on differences in the material thermal histories and annealing treatments between various studies.

### 3.5. Dielectric properties in melting and crystallisation

Crystalline tablets of the polyols were analysed with DEA. In the crystalline state, mobility of molecules was strongly restricted and it could be observed from permittivity spectra of crystalline xylitol shown in Fig. 7 as compared with permittivity spectra of amorphous xylitol shown in Fig. 8. Melting of crystalline polyols occurred at their specific melting temperatures of 118, 92 and  $97^\circ\text{C}$  for erythritol, xylitol and sorbitol, respectively, as observed from a sharp



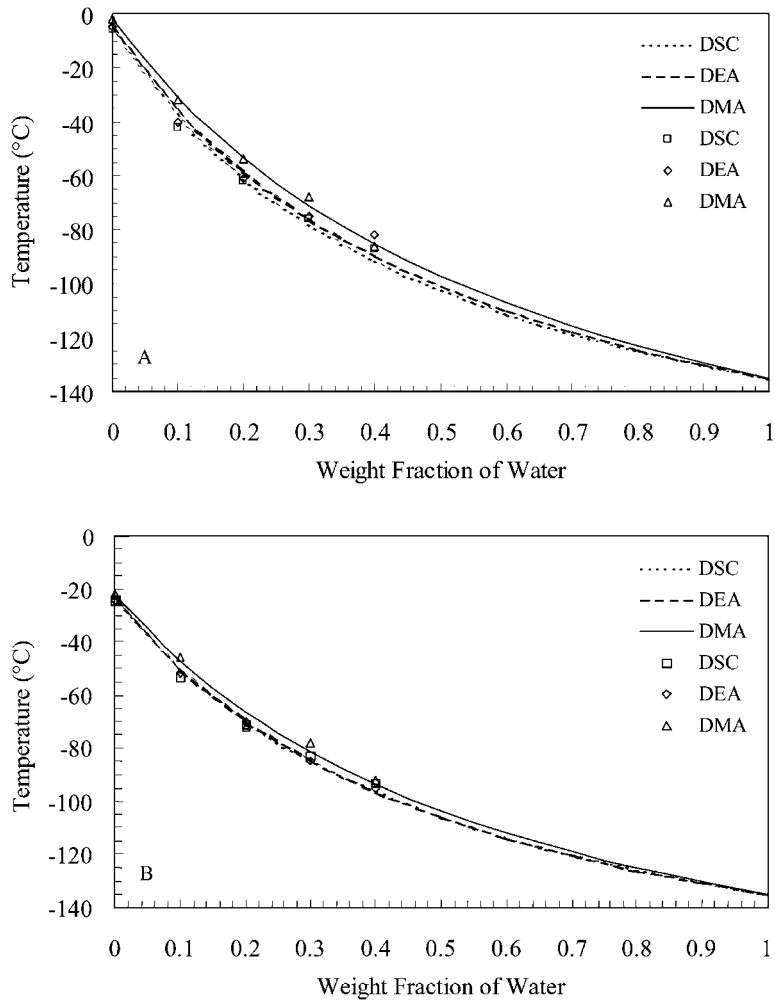


Fig. 6. Glass transition temperature ( $T_g$ ) for (A) sorbitol and (B) xylitol as a function of water content. The solid lines were predicted with the Gordon–Taylor Eq. (2) fitted to the experimental data shown.

frequency independent increase in the permittivity data (Fig. 7). In the loss factor data, a frequency independent change at the same temperature was also observed. These changes represented melting of crystals and the change in molecular mobility as the liquid phase was formed. Erythritol and xylitol melts crystallised during cooling and the  $\epsilon'$  and the  $\epsilon''$  showed no  $\alpha$ -relaxation as shown in Fig. 7. In the reheating scans, no  $\alpha$ -relaxation was apparent and the materials showed a frequency independent change at the melting temperature. Sorbitol melt remained amorphous during cooling and showed an  $\alpha$ -relaxation in the reheating scan which was comparable with that

of the completely amorphous material. In general, the polyols studied showed a high tendency for crystallisation and they can be considered as fragile liquids according to the fragile and strong classification of supercooled liquids [30].

The DSC thermogram for a mixture of crystalline and amorphous xylitol (Fig. 9) showed the glass transition at the same temperature (onset  $-24^\circ\text{C}$ ) as the anhydrous, amorphous xylitol. The glass transition was followed by a crystallisation exotherm with onset at  $37^\circ\text{C}$  and peak maximum at  $59^\circ\text{C}$ . The melting endotherm of the crystals had an onset at  $90^\circ\text{C}$ . The DEA results for xylitol melts with added xylitol

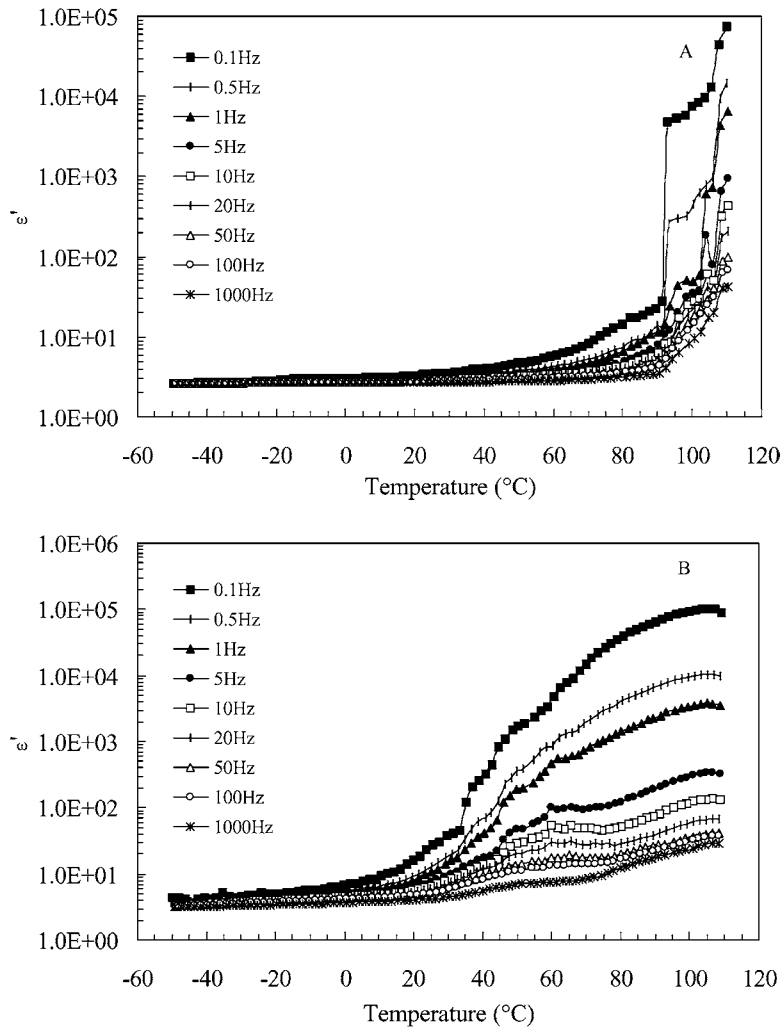


Fig. 7. Typical dielectric permittivity spectra for xylitol at various frequencies as measured during heating of (A) crystalline xylitol and (B) cooling of the xylitol melt at  $2^{\circ}\text{C min}^{-1}$ .

crystals are shown in Fig. 8. The material showed an  $\alpha$ -relaxation at a frequency-dependent temperature. Frequency independent changes were observed at around 40 and  $94^{\circ}\text{C}$  corresponding to crystallisation and melting transitions of xylitol. After crystallisation of the mixture, the permittivity and loss factor increased steadily, differing from the dielectric behaviour of amorphous xylitol. In Fig. 10, the loss modulus ( $E''$ ) is shown for the mixture as a function of temperature measured by DMA. The  $\alpha$ -relaxation was observed at a frequency-dependent temperature at

$-21^{\circ}\text{C}$  at 1 Hz. The maximum of the  $\alpha$ -relaxation peak was shifted to higher temperatures with increasing frequency. A sharp frequency independent change of loss modulus was observed with onset at around  $40^{\circ}\text{C}$ , and the sample was hard and brittle when the measurement was completed, indicating crystallisation. These changes in DEA, DMA and DSC data showed that the added xylitol crystals acted as seeds for nuclei and enhanced crystallisation. Moreover, DEA, DMA, and DSC gave complementary information about the phase and state transitions.

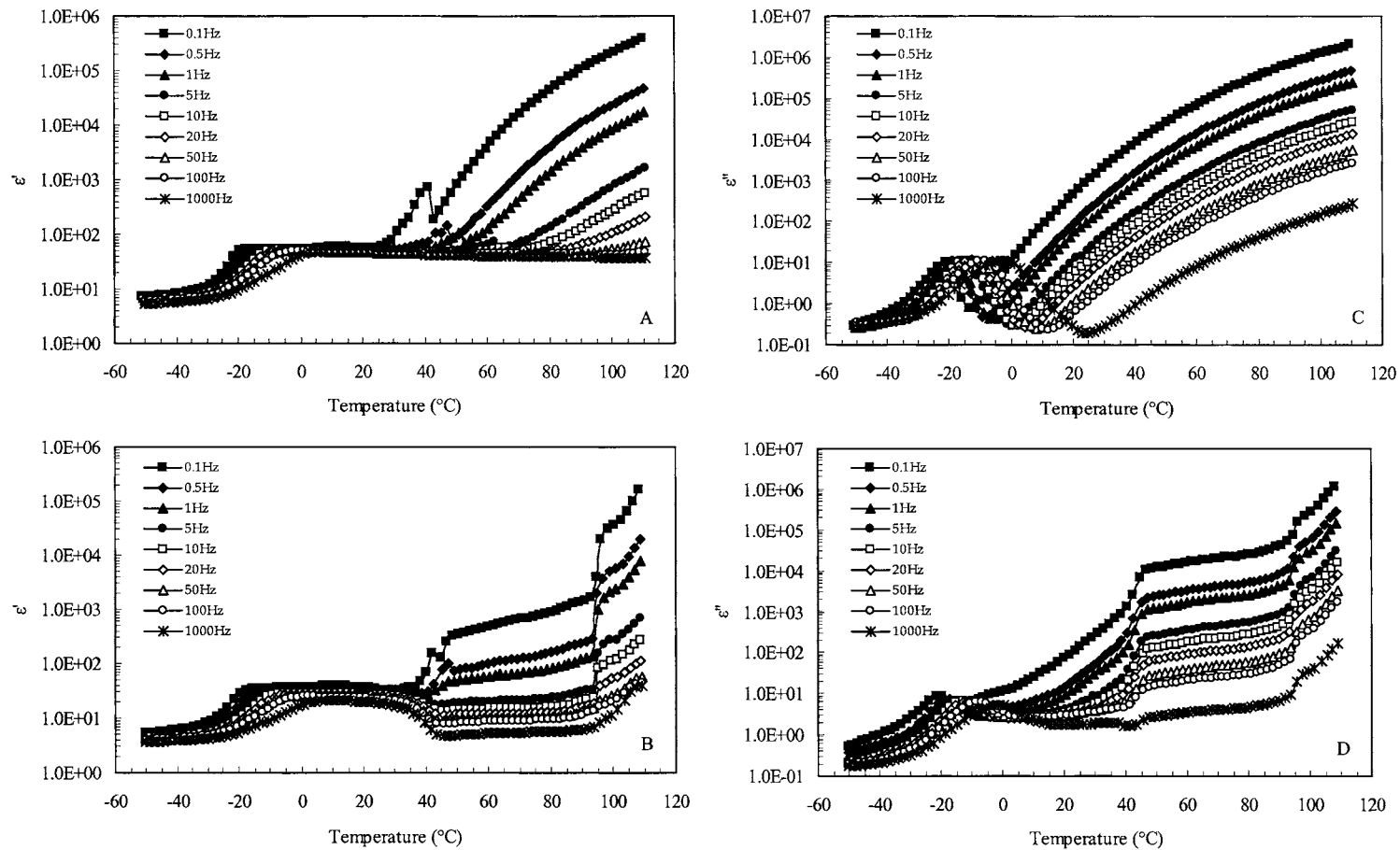


Fig. 8. Typical dielectric permittivity ( $\epsilon'$ ) and loss factor ( $\epsilon''$ ) spectra at various frequencies obtained during dynamic heating of amorphous anhydrous xylitol (A and C) and a mixture of amorphous and crystalline xylitol (B and D) at  $2^\circ\text{C min}^{-1}$ .

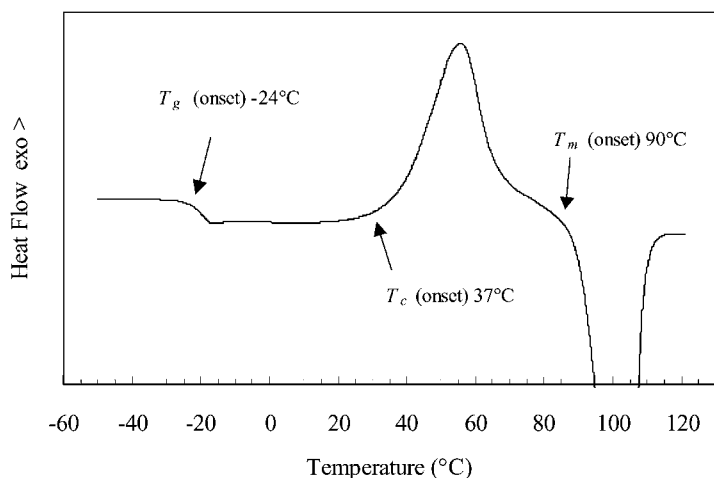


Fig. 9. Typical DSC thermogram for a mixture of amorphous (99%) and crystalline (1%) xylitol obtained using dynamic heating at  $5^{\circ}\text{C min}^{-1}$ . The glass transition,  $T_g$ , and crystallisation exotherm,  $T_c$ , of amorphous xylitol, and melting endotherm,  $T_m$ , of the crystals had onset temperatures at  $-24$ ,  $37$  and  $90^{\circ}\text{C}$ , respectively.

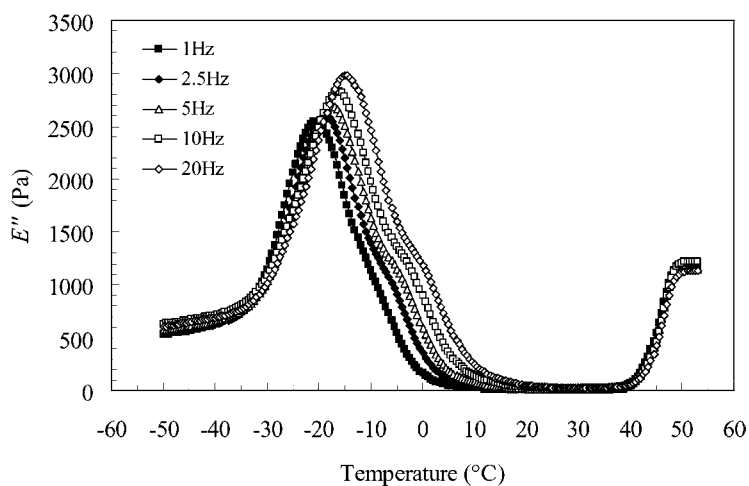


Fig. 10. Typical loss modulus ( $E''$ ) for a mixture of amorphous (99%) and crystalline (1%) xylitol at various frequencies measured using dynamic heating at  $2^{\circ}\text{C min}^{-1}$ .

#### 4. Conclusions

The glass transition temperature range of polyols decrease with increasing water content due to water plasticisation. Similar plasticisation behaviour was observed from complementary detection of changes in dielectric, mechanical, and thermal properties occurring over the glass transition. The changes in dielectric properties were also found to provide infor-

mation of changes in crystallinity and the melting transition. Xylitol crystals added to an amorphous xylitol melt were proposed to act as seeds for nuclei and enhance crystallisation from the amorphous state. These three different thermal analytical methods gave slightly different temperature values for the glass transition, crystallisation and melting of polyols at selected frequencies of 0.1 and 1 Hz for DEA and DMA, respectively.

## Acknowledgements

The study has been carried out with financial support from Leaf Inc. and TEKES, the National Technology Agency.

## References

- [1] J. Goossens, M. Gonze, *Manufac. Confect.* 80 (2000) 71.
- [2] J.M. deMan, *Principles of Food Chemistry*, Aspen Publication, Gaithersburg, MD, 1999, p. 181.
- [3] R.C. Lindsay, in: O.R. Fennema (Ed.), *Food Chemistry*, 3rd Edition, Marcel Dekker, New York, 1996, p. 793.
- [4] R.L. Whistler, J.N. BeMiller, *Carbohydrate Chemistry for Food Scientists*, Eagan Press, St. Paul, MN, 1997, p. 23.
- [5] L.H. Sperling, *Introduction to Physical Polymer Science*, 2nd Edition, Wiley, New York, 1992, p. 303.
- [6] Y.H. Roos, *Phase Transitions in Foods*, Academic Press, New York, 1995, p. 157.
- [7] G.S. Parks, S.B. Thomas, *J. Am. Chem. Soc.* 56 (1934) 1423.
- [8] A. Barkatt, C.A. Angell, *J. Chem. Phys.* 70 (1979) 901.
- [9] L. Slade, H. Levine, *Crit. Rev. Food Sci. Nutr.* 30 (1991) 115.
- [10] F. Franks, M.H. Asquith, C.C. Hammond, H.B. Skaer, P. Echlin, *J. Microsc.* 119 (1977) 223.
- [11] Y.H. Roos, *J. Thermal Anal.* 48 (1997) 535.
- [12] G. Buckton, P. Darcy, *Int. J. Pharma.* 136 (1996) 141.
- [13] Y. Roos, M. Karel, *J. Food Sci.* 57 (1992) 775.
- [14] K. Jouppila, J. Kansikas, Y.H. Roos, *Biotechnol. Prog.* 14 (1998) 347.
- [15] B. Luyet, D. Rasmussen, *Biodynamica* 10 (1968) 167.
- [16] M.J. Izzard, S. Ablett, P.J. Lillford, in: E. Dickinson (Ed.), *Food Polymers, Gels and Colloids*, The Royal Society of Chemistry, Cambridge, 1991 (Chapter 23).
- [17] Y. Roos, M. Karel, *Int. J. Food Sci. Technol.* 26 (1991) 553.
- [18] Y. Roos, *Carbohydr. Res.* 238 (1993) 39.
- [19] D.R. Lide (Ed.), *Handbook of Chemistry and Physics*, Section 3, 73rd Edition, CRC Press, Boca Raton, 1992.
- [20] W.M. MacInnes, in: J.M.V. Blanshard, P.J. Lillford (Eds.), *The Glassy State in Foods*, Nottingham University Press, Loughborough, UK, 1993, p. 223.
- [21] T.J. Laaksonen, Y.H. Roos, *J. Cereal Sci.* 32 (2000) 281.
- [22] G. Barone, G.D. Gatta, D. Ferro, V. Piacente, *J. Chem. Soc., Faraday Trans.* 86 (1990) 75.
- [23] P.D. Orford, R. Parker, S. Ring, *Carbohydr. Res.* 196 (1990) 11.
- [24] S.S.N. Murthy, *Mol. Phys.* 87 (1996) 691.
- [25] A. Raemy, T.F. Schweizer, *J. Thermal Anal.* 28 (1983) 7751.
- [26] R.J. Williams, *Ann. Bot.* 74 (1994) 525.
- [27] T.R. Noel, S.G. Ring, M.A. Whittam, *J. Phys. Chem.* 96 (1992) 5662.
- [28] M. Gordon, J.S. Taylor, *J. Appl. Chem.* 2 (1952) 493.
- [29] G.P. Johari, A. Hallbrucker, E. Mayer, *Nature (London)* 330 (1987) 552.
- [30] C.A. Angell, R.D. Bressel, J.L. Green, H. Kanno, M. Oguni, E.J. Sare, *J. Food Eng.* 22 (1994) 115.